research papers

Estimation of soft X-ray and EUV transition radiation power emitted from the MIRRORCLE-type tabletop synchrotron

N. Toyosugi,[a] H. Yamada,[a,b,c]* D. Minkov,[a] M. Morita,[a] T. Yamaguchi[c] and S. Imai[c]

[a]Photon Production Laboratory Ltd, Ritsumeikan University, 1-1-1 Nojihigashi, Kusatsu-shi, Shiga 525-8577, Japan, [b]21st Century COE Synchrotron Light Life Science Center, Ritsumeikan University, 1-1-1 Nojihigashi, Kusatsu-shi, Shiga 525-8577, Japan, and [c]Ritsumeikan University, 1-1-1 Nojihigashi, Kusatsu-shi, Shiga 525-8577, Japan. E-mail: hironari@se.ritsumei.ac.jp

The tabletop synchrotron light sources MIRRORCLE-6X and MIRRORCLE-20SX, operating at electron energies $E_{el} = 6$ MeV and $E_{el} = 20$ MeV, respectively, can emit powerful transition radiation (TR) in the extreme ultraviolet (EUV) and the soft X-ray regions. To clarify the applicability of these soft X-ray and EUV sources, the total TR power has been determined. A TR experiment was performed using a 385 nm-thick Al foil target in MIRRORCLE-6X. The angular distribution of the emitted power was measured using a detector assembly based on an NE102 scintillator, an optical bundle and a photomultiplier. The maximal measured total TR power for MIRRORCLE-6X is $P_{max} \cong 2.95$ mW at full power operation. Introduction of an analytical expression for the lifetime of the electron beam allows calculation of the emitted TR power by a tabletop synchrotron light source. Using the above measurement result, and the theoretically determined ratio between the TR power for MIRRORCLE-6X and MIRRORCLE-20SX, the total TR power for MIRRORCLE-20SX can be obtained. The one-foil TR target thickness is optimized for the 20 MeV electron energy. $P_{max} \cong 810$ mW for MIRRORCLE-20SX is obtained with a single foil of 240 nm-thick Be target. The emitted bremsstrahlung is negligible with respect to the emitted TR for optimized TR targets. From a theoretically known TR spectrum it is concluded that MIRRORCLE-20SX can emit 150 mW of photons with $E > 500$ eV, which makes it applicable as a source for performing X-ray lithography. The average wavelength, $\overline{\lambda} = 13.6$ nm, of the TR emission of MIRRORCLE-20SX, with a 200 nm Al target, could provide of the order of 1 W EUV.

Keywords: MIRRORCLE-type tabletop synchrotron; transition radiation; total soft X-ray power; total EUV power.

1. Introduction

A MIRRORCLE-type synchrotron (Yamada, 1996) emitting transition radiation (TR) represents an important source of soft X-ray and extreme ultraviolet (EUV) radiation. Such radiation can be used for performing deep-edge lithography for the LIGA process micro-fabrication (Ehrfeld & Munch-meyer, 1991), X-ray lithography (XRL) (Piestrup et al., 1985) and possibly EUV lithography (EUVL) (Shriever, 2004) for manufacturing next-generation semiconductor chips. There-fore, the development of MIRRORCLE-type sources emitting larger TR power is of significant practical interest.

Linear accelerators (LINACs) have been mostly used for emission of TR, and the maximum reported TR power emitted from a LINAC is 15.2 mW (Piestrup et al., 1991). LINACs operate at very high electron energies, $E_{el} = 100$–10000 MeV; their electrons pass only once along linear trajectories which leads to a relatively low beam current, $I_B = 1$–100 µA. More recently, storage rings have been used for emission of TR. Storage rings operate at lower electron energies, $E_{el} \simeq$ several tens of MeV, and their electrons pass many times along quasi-circular orbits, which results in a much larger I_B. Although we are not aware of any experimental data regarding TR power emitted from storage rings, it has been concluded that the expected emitted TR power should be ~ 100 mW (Piestrup et al., 1998).

In Japan, the compact storage ring Aurora (Yamada, 1990), which uses a superconducting magnet, has not gained suffi-cient recognition owing to the inconvenience of using liquid He and an insufficient I_B. A theory for the emission of bright
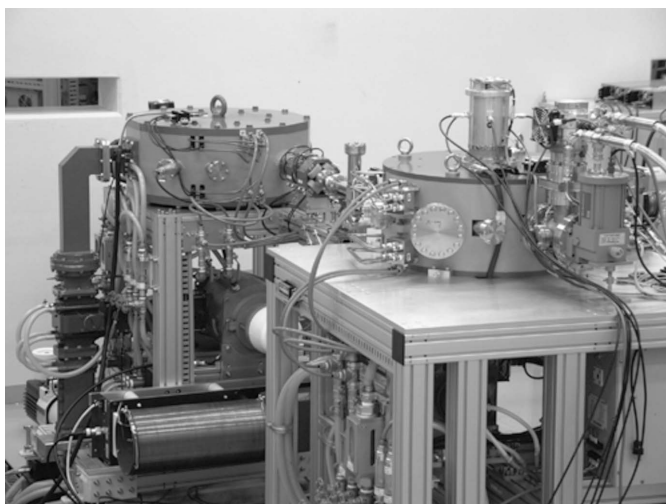
hard X-rays by MIRRORCLE-type synchrotrons (Yamada, 1996) has laid the foundation for development of the low-energy storage ring MIRRORCLE, which can operate at a very large beam current, $I_B > 1$ A. After resolving the injection problem (Yamada *et al.*, 2001), the tabletop storage ring MIRRORCLE-6X, operating at E_{el} = 6 MeV (Photon Production Laboratory, http://www.ppl-xray.com), has been developed (Hasegawa, 2004) and used for the generation of bright hard X-rays (Yamada, 2004).

MIRRORCLE-6X is suitable for performing TR experiments owing to its large beam current and compactness. Problems for its practical application as a TR source are insufficient beam lifetime and insufficient emission of TR power per electron owing to its low electron energy. Therefore, at present, we are commissioning the storage ring MIRRORCLE-20SX with E_{el} = 20 MeV (Toyosugi *et al.*, 2006).

To find out the present limitations of the applicability of MIRRORCLE as an EUV and soft X-ray source, we need to evaluate the maximum emitted TR power for both MIRRORCLE-6X and MIRRORCLE-20SX. In this paper the emitted TR power is determined in an experiment using MIRRORCLE-6X and an Al stripe TR target. Based on this experimental observation, the available total TR power is estimated for both MIRRORCLE-6X and MIRRORCLE-20SX.
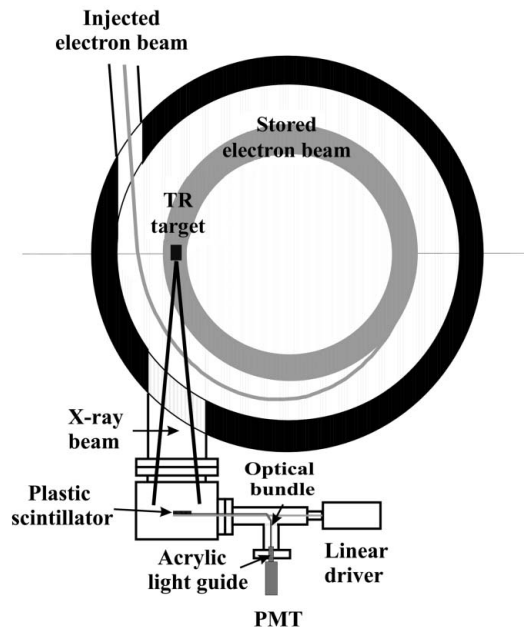
2. Experimental set-up

Our experiment was performed on MIRRORCLE-6X, which contains a 6 MeV microtron injector and storage ring (Fig. 1). The microtron injects electron pulses with a peak injected current $I_P \leq 100$ mA, an injection pulse time $T \leq 150$ ns and an injection rate $R \leq 400$ Hz (Hasegawa *et al.*, 2004). The dimensions of MIRRORCLE-6X are 1 m × 2 m × 1.5 m (http://www.ppl-xray.com). A schematic diagram of the set-up of our experiment is shown in Fig. 2.

The electron beam in the storage ring has an elliptical cross section, with a length of 20 mm along its horizontal axis and a height of 3 mm. To ensure a small square emitting area, our TR target represented a vertical stripe of one Al foil with a width of 2.5 mm. When one electron hits the target, it emits TR with a conical shape (Ter-Mikaelyan, 1961) (Fig. 3).

The detector includes a plastic scintillator (PS) made of NE102, an optical bundle and a photomultiplier (PMT). The PS is driven to points x_j located along a horizontal line, which is perpendicular to the axis of the TR emission cone and crosses it at $x = 0$. The PS is kept under the storage-ring vacuum, and there are no obstacles between it and the target. The distance between the target and the PS is 483 mm, at the

Figure 2
Set-up of our experiment for measurement of the emitted power from MIRRORCLE-6X with a TR target.

Figure 1
Photograph of the storage-ring synchrotron MIRRORCLE-6X at SLLS Ritsumeikan University.
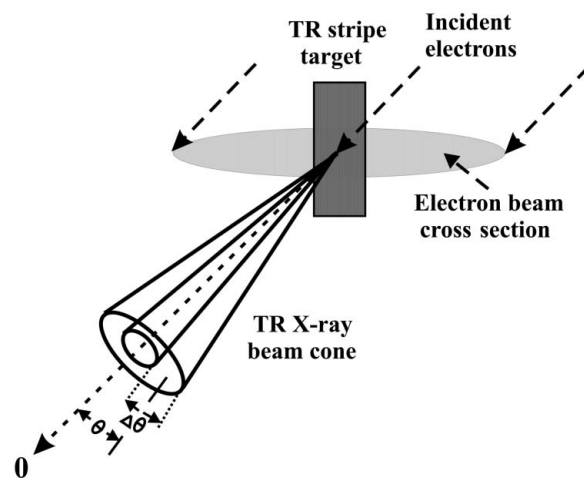
Figure 3
Illustration of the cross section of the electron beam in the storage ring, and the positioning of the TR target. TR is emitted with a conical spatial distribution, and $\theta \cong \Delta\theta$.

point $x = 0$. The current from the PMT output is recorded for each PS location.

The PS is a rectangular piece of NE102 with a surface area of 3 mm × 3 mm and a thickness of 8.5 µm. The PS is glued to a quartz substrate of dimensions 8 mm × 8 mm × 1 mm. An optical bundle of diameter 6 mm, made of 0.3 mm-diameter optical fibres, is glued to the other side of the quartz substrate. The PMT (H3165-10, Hamamatsu Photonics) is greased to the other end of the optical bundle. When illuminated by soft X-rays, NE102 emits visible light with a peak at 423 nm and a pulse width of ∼2.7 ns. H3165-10 operates at 1 kV, and its response time is ∼2.5 ns. The charge generated at the PMT output is supplied to an I–F converter, whose current output is recorded in counts, where 1 count = 10 pA.

The TR emitted from the TR target includes photons with a continuous spectrum of energies E from the EUV to the soft X-ray regions. In this paper the photon energy is counted in eV. Our detector was designed to have a maximum efficiency at $E \simeq 1000$ eV. We used the detector calibration service offered by the AIST storage-ring source to calibrate the detector in the spectral range $E = 500$–1150 eV.

3. Analytical method

The total current I_{PT} measured at the PMT output is

$$I_{PT} = (i_c/2S_0) \sum_j Y_j S_j,$$ (1)

where Y_j is the PMT output current, in counts, at the jth measurement point x_j, $i_c = 10$ pA is the current value for one count of the PMT output, $S_0 = 9 \times 10^{-6}$ m^2 is the surface area of our PS,

$$S_j = \frac{\pi d_{meas}^2}{4} \text{Abs}\left\{\left[\tan(\theta_j) + \tan(\theta_{j+1})\right]^2 - \left[\tan(\theta_j) + \tan(\theta_{j-1})\right]^2\right\}$$

is the surface area from the measurement plane limited between the circles with a centre at the point 0, where the emission cone axis crosses the measurement plane and radii $d_{meas}\text{Abs}\{[\tan(\theta_j) + \tan(\theta_{j+1})]/2\}$ and $d_{meas}\text{Abs}\{[\tan(\theta_j) + \tan(\theta_{j-1})]/2\}$, and $\theta_j = \arctan(x_j/d_{meas})$. It is assumed that, if the PS is located at any point on this surface area, the PMT output would be Y_j counts. The term 1/2 in (1) discounts the use of measurement points x_j located on both sides of the TR axis.

The measured emitted TR power for our reference experiment with MIRRORCLE-6X is

$$P_r = I_{PT} \int_{E_{min}}^{E_{max}} [f(E)/\eta(E)] \, dE,$$ (2)

where

$$f(E) = \frac{\int_{\theta=0}^{\theta_{max}} \frac{d^2N}{dE\,d\Omega} \, d\Omega}{\int_{E_{min}}^{E_{max}} \left(\int_{\theta=0}^{\theta_{max}} \frac{d^2N}{dE\,d\Omega} \, d\Omega\right) dE} = \frac{f_0(E)}{\Delta N_{ph/el}},$$

and $\eta(E)$ [A W^{-1}] is the detector efficiency. The TR cross section, $d^2N/dE\,d\Omega$, represents the number of photons emitted within the photon energy interval dE, and the axially symmetrical spatial angle $d\Omega = 2\pi \sin\theta \, d\theta$, for one pass of one electron through the target, where θ is the photon emission angle with respect to the direction of the electron. The denominator $\Delta N_{ph/el}$ is the number of emitted photons within the measured spatial angle for one pass of one electron through the target. The analytical approximation of $\eta(E)$ for our detector is derived in Appendix A.

The calculated emitted TR power is

$$P_c = N_{el/s} E_{TR/el},$$ (3)

where $N_{el/s}$ is the number of electrons passing through the TR target for 1 s and $E_{TR/el}$ is the emitted TR energy for one pass of one electron through the TR target. Formulae for calculating $N_{el/s}$ and $E_{TR/el}$ are presented in Appendices B and C, respectively. The calculated ratio R_P of the TR power P_c and P_{c2} emitted in two experiments, performed using different synchrotron operation parameters I_P, T and R, as well as different TR targets, is

$$R_P = P_c/P_{c2}.$$ (4)

If the second of the above experiments is considered to be identical to our reference experiment with MIRRORCLE-6X, the TR power P observed in the first experiment is estimated to be

$$P = P_r R_P.$$ (5)

4. Results

4.1. Experiment using MIRRORCLE-6X

Our reference experiment was performed using MIRRORCLE-6X with operating conditions $I_P = 40$ mA, $T = 100$ ns and $R = 200$ Hz. The TR target was one Al foil stripe of width 2.5 mm, height 15 mm and thickness $d = 385$ nm. Two experiments were conducted, with and without a target, by moving the TR target in and out of the electron beam. The measured dependence of the PMT output current count Y as a function of the emission angle θ is shown in Fig. 4 for both cases.

4.2. Comparison between experimental and calculated results for MIRRORCLE-6X

The difference between the above PMT output current counts with and without a target represents the measured angular dependence of the target emission. The measured and calculated angular dependencies for both TR and bremsstrahlung (BR) are shown in Fig. 5 for the above experimental conditions.

The shape of the measured angular dependence is similar to that of TR, with two similar magnitude maxima at $\pm\theta_{max} = 40$ mrad. The significant difference between the measured and the calculated results is ascribed to the presence of a magnetic

Table 1
Characteristics of the experimental conditions, and the calculated emitted power.

The first data line shows the results from our experiments. The asterisks (*) in the fifth column indicate the maximum possible total TR power which can be emitted from the present scheme MIRRORCLE-6X and 20SX.

Storage-ring synchrotron	Injected beam current I_{Bi} (μA)	One-foil TR target	Average beam current I_B (A)	Emitted TR power P (mW)	Emitted BR power P_{Br} (mW)	Emitted TR power $P_{E>500\,eV}$ (mW)	Average photon wavelength $\bar{\lambda}$ (nm)
MIRRORCLE-6X experiment	0.8	385 nm Al	0.012	0.394	0.0022	0.0128	26.7
MIRRORCLE-6X	6.0	35 nm C	2.09	65.6*	0.0092	1.42	37.9
MIRRORCLE-20SX	6.0	200 nm Al	0.69	288.3	0.1377	63.9	13.6
MIRRORCLE-20SX	6.0	220 nm C	1.63	606.9	0.0846	132.0	12.1
MIRRORCLE-20SX	6.0	240 nm Be	2.32	811.6*	0.0642	151.2	10.9
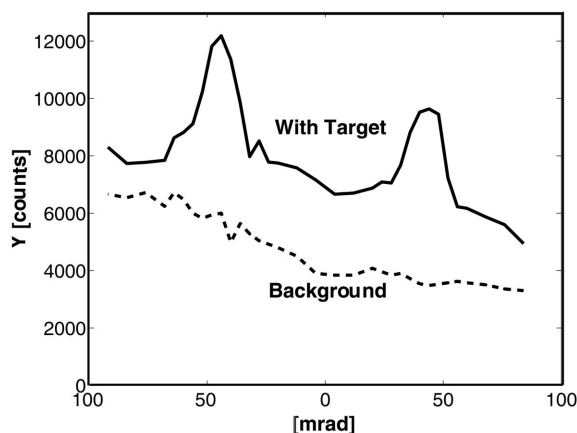
Figure 4
Measured dependence of the PMT output current count Y as a function of the emission angle θ, with and without a target (background). The experiment was performed using MIRRORCLE-6X at $I_P = 40$ mA, $T \cong 100$ ns and $R = 200$ Hz. The TR target was a 2.5 mm-wide Al foil stripe of thickness $d = 385$ nm. The PMT was operated at 1 kV.
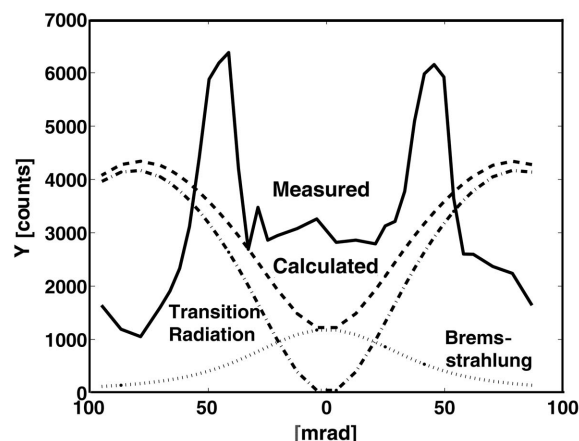
Figure 5
Comparison between the measured and calculated angular dependencies for emission of TR and BR. The measured dependence is the difference between the PMT output without and with a target from Fig. 4. The calculations are performed for the same experimental conditions of MIRRORCLE-6X.

field $B = 0.1282$ T at the target in MIRRORCLE-6X. This magnetic field provides motion of the relativistic electrons along an almost circular orbit. It also limits the motion of atomic electrons in the target during the generation of TR, and leads to a smaller measured value of θ_{max} compared with its calculated value. The theoretical study of TR under a magnetic field is necessary in order to clarify this difference for further investigation, but is not reported here. Whether TR is enhanced or suppressed by the magnetic field, and whether the TR distribution is compressed by the magnetic field are interesting points to be studied.

It is assumed that approximately 15% of TR is emitted at angles $\theta > \theta_{max}$ for this experiment. Therefore, the total emitted TR power is $P_r \cong 394$ μW, and the total emitted BR power is $P_{BR} \cong 2.2$ μW. At full-power operation (at 100 mA and 400 Hz injection rate), $P_r \cong 2.95$ mW should be obtained.

4.3. Estimation of the practically available TR power emitted from MIRRORCLE-6X and MIRRORCLE-20SX

The full-power operating conditions of MIRRORCLE-6X and MIRRORCLE-20SX are $I_P = 100$ mA, $T = 150$ ns and $R =$

400 Hz. The design of TR targets optimized for performing XRL using MIRRORCLE was investigated by Minkov *et al.* (2006*a*). It was concluded there that the best one-chemical element TR target for performing XRL using MIRRORCLE-6X contains one C foil of thickness $d = 35$ nm. The best one-chemical element TR target for performing XRL using MIRRORCLE-20SX contains one foil of (*a*) Be with $d = 240$ nm, (*b*) C with $d = 220$ nm or (*c*) Al with $d = 200$ nm.

The ratio R_P is calculated next from equation (4), for these optimum TR experiments with MIRRORCLE-6X and MIRRORCLE-20SX. The maximum emitted TR power is estimated from (5). In spite of the significant difference between the experimental and the theoretical angular distributions of the target emission for our MIRRORCLE-6X experiment, we use (5) for estimation of emitted TR power from MIRRORCLE-20SX because our first TR experiments with the 20 MeV machine show that the ratio between the measured θ_{max} and its theoretical value is almost the same for the MIRRORCLE-6X and MIRRORCLE-20SX experiments. Since only photons with energy $E > 500$ eV can be used for performing XRL, the emitted power of such photons is also calculated. All obtained results are included in Table 1.
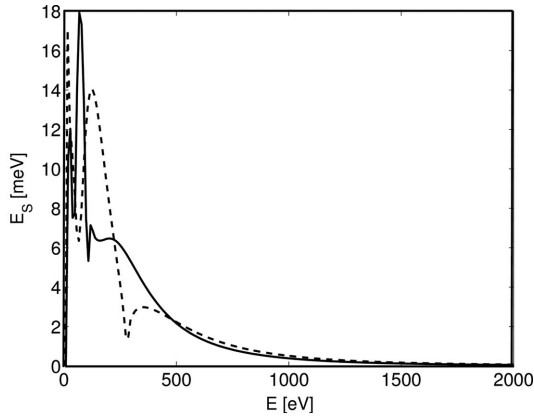
Figure 6
Spectral dependence $E_S(E)$ (see text) of the TR energy emitted within 1 eV around the photon energy E for one pass of one electron through one 220 nm-thick C foil (dashed line) and one 240 nm-thick Be foil (solid line) in MIRRORCLE-20SX.

The spectral dependence

$$E_S(E) = E \left(\int_\theta \frac{\mathrm{d}^2 N}{\mathrm{d}E \, \mathrm{d}\Omega_{|E}} \, \mathrm{d}\Omega \right) \times 1 \, \mathrm{eV}$$

of the emitted TR energy from MIRRORCLE-20SX for one 240 nm Be foil TR target and for one 220 nm C foil TR target is shown in Fig. 6. $E_S(E)$ is the number of emitted TR photons with energies $[E - 0.5 \, \mathrm{eV}, E + 0.5 \, \mathrm{eV}]$ for one incidence of one electron multiplied by E.

5. Discussion

The introduction of an explicit analytical expression for the beam lifetime τ [see equation (7) in Appendix B] allows calculation of the emitted TR power P by a storage ring for the first time. This cannot be done using the theory of TR emission by low-energy storage rings (Minkov *et al.*, 2006b) alone, where τ depends on an unknown constant.

The results obtained from this work show that a TR power of $P = 65$ mW can be emitted using a 35 nm-thick C-foil target from MIRRORCLE-6X, and $P = 810$ mW can be emitted using a 240 nm-thick Be foil from MIRRORCLE-20SX. Since at least 10 mW power of photons with $E > 500$ eV is needed for performing XRL (Piestrup *et al.*, 1985), MIRRORCLE-6X cannot be used, but MIRRORCLE-20SX can be used comfortably. An EUV source with $\bar{\lambda} = 13$–14 nm is required for EUVL (Shriever, 2004). Therefore, MIRRORCLE-20SX, with a 200 nm-thick Al target, can be considered as a possible source for performing EUVL.

The expected emission of such a large TR power from MIRRORCLE-20SX is due to the large lifetime τ and the small circulation radius r_0 of the electrons injected into the storage ring. Furthermore, the very large dynamic aperture of MIRRORCLE leads to a long lifetime τ due to the 1 cm vertical half-chamber aperture (Yamada, 1996).

The significant difference between the measured and the calculated angular dependencies of the PMT output current count for our MIRRORCLE-6X experiment indicates that the storage-ring magnetic field strongly influences the TR emission, decreasing the emitted power. Since there has been no study of the influence of the magnetic field on the emission of TR, such a study must be of interest for our future work.

APPENDIX A
Detector efficiency

The quantum efficiency of our detector, $\eta_0(E) = \eta(E) E \times 1.602 \times 10^{-19}$ (C photon^{-1}), is determined by the spectral response of the NE102 PS, and is approximated analytically over the entire emitted TR spectrum to fit to its calibration data. The low-energy region of NE102 is modelled by analogy with that of $La_{1.996}Tm_{0.004}O_2S$ resulting from their similar energy conversion efficiencies (3% for NE102 and 3.6% for $La_{1.996}Tm_{0.004}O_2S$). The large diffusion lengths of generated carriers, ~ 45 nm, are due to a lower concentration of scintillating centres and a medium level of surface recombination, ~ 10. $La_{1.996}Tm_{0.004}O_2S$ has a plasma energy $E_{pl} \cong 19.4$ eV. Its quantum efficiency at $E \leq 25$ eV has a small slope limited by surface recombination, and $\eta_0 (E \leq 25 \, \mathrm{eV}) \cong \eta_0 (100 \, \mathrm{eV})/13 \times E/25$ (Benitez *et al.*, 1991). For NE102, $E_{pl} \cong 16.15$ eV and non-radiation surface recombination should dominate at $E \leq 16.15 \times 25/19.40 = 20.8$ eV. According to the definition of $\eta_0(E)$, it should also increase linearly for $E > 20.8$ eV but with a larger slope. For much higher photon energies, only a decreasing part of the incident TR is absorbed in NE102, which leads to decreasing $\eta_0(E)$ with E. Therefore, our detector efficiency is approximated as follows,

$$\eta(E) \left[\frac{A}{W} \right] = \begin{vmatrix} \frac{\eta_0 \, (100 \, \mathrm{eV})}{(13 \times 20.8 \times 1.602 \times 10^{-19})} & \text{for } E \leq 20.8 \, \mathrm{eV} \\ \max \left\{ \eta \, (20.8 \, \mathrm{eV}), \frac{0.2764(E - 20.8)\{1 - \exp[-\mu_{PS}(E)d_{PS}]\}}{E} \right\} \\ & \text{for } E > 20.8 \, \mathrm{eV} \end{vmatrix} \quad (6)$$

where $\mu_{PS}(E)$ and $d_{PS} = 8.5$ μm are the linear absorption coefficient and the thickness of our NE102 PS, respectively, and the term in the large brackets describes the absorption of TR in the NE102 PS. The coefficient 0.2764 in the expression for $E > 20.8$ eV is introduced in order to fit the analytical dependence to the calibration data. Both the calibration data and the analytical approximation of the quantum efficiency of our detector, $\eta_0(E)$, are shown in Fig. 7.

APPENDIX B
Lifetime of the injected electrons and their number of electron passes through the target for 1 s

In both MIRRORCLE-6X and MIRRORCLE-20SX the injected electrons move along almost perfectly circular orbits with a radius $r_0 = 155.8$ mm. The beam width is 20 mm in MIRRORCLR-6X and 10 mm in MIRRORCLE-20SX, and
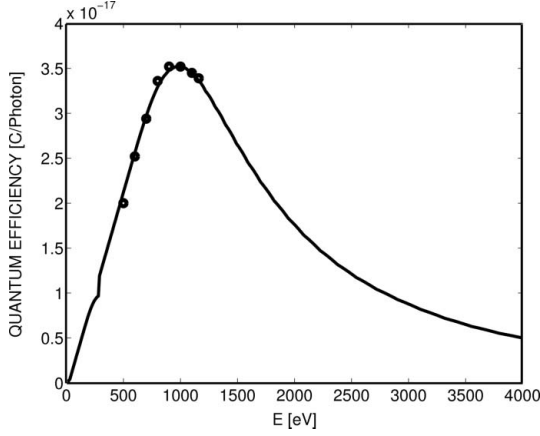
Figure 7
Spectral dependence of the quantum efficiency $\eta_0(E)$ of our detector. Circles: calibrated data; line: our analytical approximation of these data. The detector includes an 8.5 µm-thick NE102 plastic scintillator, an optical bundle of diameter 6 mm, and a H3165-10 photomultiplier (Hamamatsu Photonics) operated at 1 kV.

the beam height is 3 mm for both. The lifetime τ of the electron beam in the storage ring is given by (Yamada, 1996)

$$\tau = \frac{137}{4r_e^2 Z^2} \left\{ \frac{2\gamma^2}{137\pi}\left(\frac{b_\perp}{\beta_\perp}\right)^2 + \frac{3}{4\left[\ln\left(\frac{183}{Z^{1/3}}\right)\right]\left[\ln\left(\frac{1}{(\Delta p/p)_{max}} - \frac{5}{8}\right)\right]} \right\}$$
$$\times \frac{\Delta t A}{R_s N_A \rho d}, \tag{7}$$

where $b_\perp$ and $\beta_\perp$ are the half-chamber aperture and the average β-function of the storage ring in either the horizontal or the vertical transverse direction, whichever is more lifetime limiting. $(\Delta p/p)_{max}$ is the half-momentum aperture of the ring, γ is the relativistic factor, and d, ρ, A and Z are the thickness, density, atomic weight and the atomic number of the foil material. $R_s = S_T/S_B$ is the ratio between the area of the target hit by the beam and the beam cross section, $\Delta t = 2\pi r_0/c$ is the time for completion of one turn of an electron in the storage ring, r_e is the classical electron radius and N_A is the Avogadro constant. $(\Delta p/p)_{max} = 0.333$ for MIRRORCLE-6X and $(\Delta p/p)_{max} = 0.2$ for MIRRORCLE-20SX, while $\beta_z = 0.1835$ m, and $b_z = 0.01$ m for both of them (Yamada, 2005). For light material targets, τ is limited by elastic scattering along the vertical direction, described by the first addend in (7).

The average beam current is given by (Yamada, 1996)

$$I_B = \frac{I_p R T \tau}{\Delta t}[1 - \exp(-1/R\tau)], \tag{8}$$

while the beam current injected in the storage ring is $I_{Bi} = I_P RT$. The number of electrons passing through the target for 1 s is given by (Yamada, 2003)

$$N_{el/s} = \frac{I_B R_s}{1.6022 \times 10^{-19}}. \tag{9}$$

APPENDIX C
Emitted TR energy for one pass of one electron through the target

The theory of TR emission from low-energy storage rings was developed (Minkov et al., 2006b) based on the theory for TR emission from LINACs (Okazaki et al., 2004). It points out that thin foil TR targets emit most TR power, and more TR power is emitted from one-foil TR targets compared with multi-foil targets. The TR cross section for a low-energy storage ring and a one-foil TR target is (Minkov et al., 2006b)

$$\frac{d^2 N}{d\Omega\, dE} = F_s F_i$$
$$= \left\{ \frac{4\alpha \sin^2\theta}{\pi^2 E} \frac{(\delta^2 + \beta^2)}{[(1/\gamma^2 + \theta^2 + 2\delta)^2 + (2\beta)^2](1/\gamma^2 + \theta^2)^2} \right\}$$
$$\times \left\{ [1 - \exp(-E\beta d/\hbar c)]^2 + 4\exp(-E\beta d/\hbar c) \right.$$
$$\left. \times \sin^2\left[(Ed/4\hbar c)(1/\gamma^2 + \theta^2 + 2\delta)\right] \right\} \tag{10}$$

where F_s gives the TR contribution from one interface foil/vacuum, and F_i formulates the TR interference between the two emitting interfaces of the foil. The dielectric constant of the foil, $\varepsilon(E) = 1 - 2[\delta(E) - i\beta(E)]$, is calculated from the known complex scattering factor of the material (Attwood, 1999).

The emitted TR energy for one incidence of one electron on the TR target is

$$E_{TR/el} = \int_{E_{min}}^{E_{max}} E\left(\int_\theta \frac{d^2 N}{dE\, d\Omega}\, d\Omega\right) dE$$
$$= \sum_{k=1}^{k=E_{max}-E_{min}} E_k\left(\int_\theta \frac{d^2 N}{dE\, d\Omega}\Big|_{E=E_k}\, d\Omega\right) \times (1\,\text{eV})$$
$$= \sum_{k=1}^{k=E_{max}-E_{min}} E_S(k), \tag{11}$$

where $E_S(E)$ is the spectral dependence of the emitted TR energy for one incidence of one electron on the target.

Taking into account that the TR cross section decreases strongly at higher energy of the emitted photons, the upper limit of the photon energy integrals in (2) and (11) is chosen to be $E_{max} = 4000$ eV. It is known that radiation with energy below the plasma energy E_{pl} of a given material is absorbed strongly in that material (Attwood, 1999). For the light TR target materials of our interest, $E_{pl}(\text{Al}) = 15.8$ eV, $E_{pl}(\text{C}) = 22.3$ eV and $E_{pl}(\text{Be}) = 18.5$ eV. Nevertheless, the lower limit of the photon energy integrals in (2) and (11) is chosen to be the minimum energy for which there are literature data about the complex scattering factor of these materials (National Institute of Standards and Technology, http://physics.nist.gov/PhysRefData/FFast/html/form.html). Therefore, we use $E_{min}(\text{Al}) = 8.5$ eV, $E_{min}(\text{C}) = 6.5$ eV and $E_{min}(\text{Be}) = 8.5$ eV.

The average wavelength of the emitted TR power is calculated as (Attwood, 1999)

$$\overline{\lambda}\,(\text{nm}) = 1239.84/\overline{E}\,(\text{eV}),$$

where

$$\overline{E} = \int\limits_{E_{\min}}^{E_{\max}} E\left(\int\limits_{\theta} \frac{\mathrm{d}^2 N}{\mathrm{d}E\,\mathrm{d}\Omega}\,\mathrm{d}\Omega\right)\mathrm{d}E \Big/ \int\limits_{E_{\min}}^{E_{\max}} \left(\int\limits_{\theta} \frac{\mathrm{d}^2 N}{\mathrm{d}E\,\mathrm{d}\Omega}\,\mathrm{d}\Omega\right)\mathrm{d}E. \tag{12}$$

APPENDIX D
Bremsstrahlung cross section

Bremsstrahlung (BR) emission from the TR target is also accounted for. It is known that, for electrons with $E_{\mathrm{el}} = E_{\mathrm{el0}} = 0.511$ MeV, BR emission is described by the 'non-screening approximation' of the target nucleus potential, as well as that, for electrons with $E_{\mathrm{el}} \geq E_{\mathrm{el\_cs}} = (192/Z^{1/3})E_{\mathrm{el0}}$, BR emission is described by the 'compete screening approximation' of the nucleus potential (Jackson, 1999). Therefore, the BR cross section is approximated as (Yamada, 1996)

$$\begin{aligned}\frac{\mathrm{d}^2 N_{\mathrm{BR}}}{\mathrm{d}E\,\mathrm{d}\Omega} &= \frac{E_{\mathrm{el\_cs}} - E_{\mathrm{el}}}{E_{\mathrm{el\_cs}} - E_{\mathrm{el0}}}\frac{\mathrm{d}^2 N_{\mathrm{BR\_ns}}}{\mathrm{d}E\,\mathrm{d}\Omega} + \frac{E_{\mathrm{el}} - E_{\mathrm{el0}}}{E_{\mathrm{el\_cs}} - E_{\mathrm{el0}}}\frac{\mathrm{d}^2 N_{\mathrm{BR\_cs}}}{\mathrm{d}E\,\mathrm{d}\Omega} \\ &= \left[\left(\frac{E_{\mathrm{el\_cs}} - E_{\mathrm{el}}}{E_{\mathrm{el\_cs}} - E_{\mathrm{el0}}}\right)\ln\left(\frac{2\gamma E_{\mathrm{el}}}{E} - \frac{1}{2}\right) + \left(\frac{E_{\mathrm{el}} - E_{\mathrm{el0}}}{E_{\mathrm{el\_cs}} - E_{\mathrm{el0}}}\right)\right. \\ &\quad\left.\times \ln\left(\frac{233}{Z^{1/3}}\right)\right]\frac{8\alpha}{137\pi E}(r_e Z\gamma)^2\frac{1 + \gamma^4\theta^4}{(1 + \gamma^2\theta^2)^4}, \end{aligned} \tag{13}$$

where N_{BR}, $N_{\mathrm{BR\_ns}}$ and $N_{\mathrm{BR\_cs}}$ are the number of BR emitted photons, number of BR photons emitted by a non-screened nucleus potential and number of BR photons emitted by a completely screened nucleus potential, respectively, for one pass of one electron through the target. For the Al target, $E_{\mathrm{el\_cs}} = 41.7$ MeV.

References

Attwood, D. (1999). *Soft X-rays and Extreme Ultraviolet Radiation*, pp. 52–61. Cambridge University Press.

Benitez, E. L., Husk, D. E., Schnatterly, S. E. & Tarrio, C. (1991). *J. Appl. Phys.* **70**, 3256–3260.

Ehrfeld, W. & Munchmeyer, D. (1991). *Nucl. Instrum. Methods*, A**303**, 523–531.

Hasegawa, D., Yamada, H., Kleev, A. I., Toyosugi, N., Hayashi, T., Yamada, T., Tohyama, I., Ro, Y. D. (2004). *Portable Synchrotron Light Sources and Advanced Applications, AIP Conference Proceedings 716*, pp. 116–119. Melville, NY: AIP Press.

Jackson, J. D. (1999). *Classical Electrodynamics.* New York: John Wiley and Sons.

Minkov, D., Yamada, H., Toyosugi, N., Yamaguchi, T., Kadono, T. & Morita, M. (2006*a*). *Appl. Phys. B*, **86**, 19–23.

Minkov, D., Yamada, H., Toyosugi, N., Yamaguchi, T., Y., Kadono, T. & Morita, M. (2006*b*). *J. Synchrotron Rad.* **13**, 336–342.

Okazaki, Y., Toyosugi, N., Yamada, H., Narazaki, Y., Takashima, T. & Imai, S. (2004). *Portable Synchrotron Light Sources and Advanced Applications, AIP Conference Proceedings 716*, pp. 124–127. Melville, NY: AIP Press.

Piestrup, M. A., Boyers, D. G., Pincus, C. I., Harris, J. L., Caplan, H. S., Silzer, R. M. & Skopik, D. M. (1991). *Appl. Phys. Lett.* **59**, 189–191.

Piestrup, M. A., Kephart, J. O., Park, H., Klein, R. K., Pantell, R. H., Ebert, P. J., Moran, M. J., Dahling B. A. & Berman, B. L. (1985). *Phys. Rev. A*, **32**, 917–927.

Piestrup, M. A., Powell, M. W., Cremer, J. T., Lombardo, L. W., Kaplin, V. V., Mihal'chuk, A. A., Uglov, S. R., Zabaev, V. N., Skopik, D. M., Silzer, R. M. & Retzlaff, G. A. (1998). *Proc. SPIE*, **3331**, 450–463.

Shriever, G. (2004). *XUV Technologies and Applications*, 326th Heraeus Seminar, Bad Honnef, Germany, 7–9 June 2004.

Ter-Mikaelyan, M. L. (1961). *Nucl. Phys.* **24**, 43–61.

Toyosugi, N., Yamada, H., Noh, Y. D., Hasegawa, D., Hayashi, T. & Minkov, D. (2006). *Ninth International Conference on Synchrotron Radiation Instrumentation (SRI 2006)*, Daegu, Korea. Abstract 21.

Yamada, H. (1990). *J. Vac. Sci. Technol. B*, **8**, 1628–1631.

Yamada, H. (1996). *Jpn. J. Appl. Phys.* **35**, L182–L185.

Yamada, H. (2003). *Nucl. Instrum. Methods*, B**199**, 509–516.

Yamada, H. (2004). *Portable Synchrotron Light Sources and Advanced Applications, AIP Conference Proceedings 716*, pp. 12–17. Melville, NY: AIP Press.

Yamada, H. (2005). *Oyo Butsuri*, **74**, 462–471.

Yamada, H., Kitazawa, Y., Kanai, Y., Tohyama, I., Ozaki, T., Sakai, Y., Kleev, A. I. & Bogomolov, G. D. (2001). *Nucl. Instrum. Methods*, A**467–468**, 122–125.